

Type I interferon susceptibility distinguishes SARS-CoV-2 from SARS-CoV.

Kumari G. Lokugamage^{1*}, Adam Hage^{1*}, Maren de Vries³, Ana M. Valero-Jimenez³, Craig Schindewolf¹, Meike Dittmann³, Ricardo Rajsbaum^{1,2}, Vineet D. Menachery^{1,2}

¹Department of Microbiology and Immunology, ²Institute for Human Infection and Immunity, University of Texas Medical Branch, Galveston TX, USA

³Department of Microbiology, New York University School of Medicine, New York, NY 10016, USA

*Equal contributions

Corresponding Author: Vineet D. Menachery

Address: University of Texas Medical Branch, 301 University Blvd, Route #0610 Galveston, TX 77555

Email: Vimenach@utmb.edu

Article Summary: SARS-CoV-2 has similar replication kinetics to SARS-CoV, but demonstrates significant sensitivity to type I interferon treatment.

Running title: SARS-CoV-2 sensitive to type I IFN pretreatment

Keywords: Coronavirus, 2019-nCoV, SARS-CoV-2, COVID-19, SARS-CoV, type I interferon, IFN

1 **Abstract**

2 SARS-CoV-2, a novel coronavirus (CoV) that causes COVID-19, has recently emerged causing
3 an ongoing outbreak of viral pneumonia around the world. While distinct from SARS-CoV, both
4 group 2B CoVs share similar genome organization, origins to bat CoVs, and an arsenal of
5 immune antagonists. In this report, we evaluate type-I interferon (IFN-I) sensitivity of SARS-
6 CoV-2 relative to the original SARS-CoV. Our results indicate that while SARS-CoV-2
7 maintains similar viral replication to SARS-CoV, the novel CoV is much more sensitive to IFN-I.
8 In Vero and in Calu3 cells, SARS-CoV-2 is substantially attenuated in the context of IFN-I
9 pretreatment, while SARS-CoV is not. In line with these findings, SARS-CoV-2 fails to
10 counteract phosphorylation of STAT1 and expression of ISG proteins, while SARS-CoV is able
11 to suppress both. Comparing SARS-CoV-2 and influenza A virus in human airway epithelial
12 cultures (HAEC), we observe the absence of IFN-I stimulation by SARS-CoV-2 alone, but detect
13 failure to counteract STAT1 phosphorylation upon IFN-I pretreatment resulting in near ablation
14 of SARS-CoV-2 infection. Next, we evaluated IFN-I treatment post infection and found SARS-
15 CoV-2 was sensitive even after establishing infection. Finally, we examined homology between
16 SARS-CoV and SARS-CoV-2 in viral proteins shown to be interferon antagonists. The absence
17 of an equivalent open reading frame (ORF) 3b and changes to ORF6 suggest the two key IFN-I
18 antagonists may not maintain equivalent function in SARS-CoV-2. Together, the results identify
19 key differences in susceptibility to IFN-I responses between SARS-CoV and SARS-CoV-2 that
20 may help inform disease progression, treatment options, and animal model development.

21 **Importance**

22 With the ongoing outbreak of COVID-19, differences between SARS-CoV-2 and the original
23 SARS-CoV could be leveraged to inform disease progression and eventual treatment options.
24 In addition, these findings could have key implications for animal model development as well as
25 further research into how SARS-CoV-2 modulates the type I IFN response early during
26 infection.

27 **Introduction**

28 At the end of 2019, a cluster of patients in Hubei Province, China was diagnosed with a
29 viral pneumonia of unknown origins. With community links to the Huanan seafood market in
30 Wuhan, the disease cluster had echoes of the severe acute respiratory syndrome coronavirus
31 (SARS-CoV) outbreak that emerged at the beginning of the century (1). The 2019 etiologic
32 agent was identified as a novel coronavirus, 2019-nCoV, and subsequently renamed SARS-
33 CoV-2 (2). The new virus has nearly 80% nucleotide identity to the original SARS-CoV and the
34 corresponding CoV disease, COVID-19, has many of the hallmarks of SARS-CoV disease
35 including fever, breathing difficulty, bilateral lung infiltration, and death in the most extreme
36 cases (3, 4). In addition, the most severe SARS-CoV-2 disease corresponded to old age (>50
37 years old), health status, and healthcare workers, similar to both SARS- and MERS-CoV (5).
38 Together, the results indicate SARS-CoV-2 infection and disease have strong similarity to the
39 original SARS-CoV epidemic occurring nearly two decades earlier.

40 In the wake of the outbreak, major research efforts have sought to rapidly characterize
41 the novel CoV to aid in treatment and control. Initial modeling studies predicted (6) and
42 subsequent cell culture studies confirmed that spike protein of SARS-CoV-2 utilizes human
43 angiotensin converting enzyme 2 (ACE2) for entry, the same receptor as SARS-CoV (7, 8).
44 Extensive case studies indicated a similar range of disease onset and severe symptoms seen
45 with SARS-CoV (5). Notably, less severe SARS-CoV-2 cases have also been observed and
46 were not captured in the original SARS-CoV outbreak. Importantly, screening and treatment
47 guidance has relied on previous CoV data generated with SARS-CoV and MERS-CoV.
48 Treatments with both protease inhibitors and type-I interferon (IFN-I) have been employed (4);
49 similarly, remdesivir, a drug targeting viral polymerases, has been reported to have efficacy
50 against SARS-CoV-2 similar to findings with both SARS- and MERS-CoV (9-12). Importantly,
51 several vaccine efforts have been initiated with a focus on the SARS-CoV-2 spike protein as the

52 major antigenic determinant (13). Together, the similarities with SARS-CoV have been useful in
53 responding to the newest CoV outbreak.

54 The host innate immune response is initiated when viral products are recognized by host
55 cell pattern recognition receptors, including Toll-like receptors (TLRs) and RIG-I-like receptors
56 (RLRs) (14, 15). This response ultimately results in production of IFN-I and other cytokines,
57 which together are essential for an effective antiviral response (16). IFN-I then triggers its own
58 signaling cascade via its receptor, in an autocrine or paracrine manner, which induces
59 phosphorylation of signal transducers and activators of transcription 1 (STAT1) and STAT2.
60 Together, STAT1, STAT2, and a third transcription factor, IRF9, form the Interferon Stimulated
61 Gene Factor 3 (ISGF3) complex, which is essential for induction of many IFN-stimulated genes
62 (ISGs), and ultimately elicit an effective antiviral response (17, 18). To establish productive
63 replication, viruses have developed different mechanisms to escape this antiviral response
64 targeting different parts of the IFN-I response machinery (19).

65 In this study, we further characterize SARS-CoV-2 and compare it to the original SARS-
66 CoV. Using Vero E6 cells, we demonstrate that SARS-CoV-2 maintains similar viral replication
67 kinetics as SARS-CoV following a low dose infection. In contrast, we find that SARS-CoV-2 is
68 significantly more sensitive to IFN-I pretreatment as compared to SARS-CoV. Infection of IFN-I
69 competent Calu3 2B4 cells resulted in reduced SARS-CoV-2 replication compared to SARS-
70 CoV. Similar to Vero cells, Calu3 cells pretreated with IFN-I had a greater reduction of
71 replication of SARS-CoV-2 compared to SARS-CoV. In human airway epithelial cultures, SARS-
72 CoV-2 showed robust replication and an absence of IFN-I stimulation contrasting influenza A
73 virus. However, pretreatment with IFN-I confirmed SARS-CoV-2 sensitivity and inability to
74 control IFN-I responses once initiated. These results suggest distinct changes between SARS-
75 CoV and SARS-CoV-2 in terms of IFN-I antagonism and we subsequently examined sequence
76 homology between the SARS-CoV and SARS-CoV-2 viral proteins that may be responsible for

77 these differences. Together, the results suggest SARS-CoV-2 lacks the same capacity to
78 control the IFN-I response as SARS-CoV.

79 **Results**

80 **SARS-CoV-2 is sensitive to IFN-I pre-treatment**

81 Our initial studies infected Vero E6 cells using a low multiplicity of infection (MOI) to
82 explore the viral replication kinetics of SARS-CoV-2 relative to SARS-CoV. Following infection,
83 we found that both SARS-CoV and SARS-CoV-2 replicate with similar kinetics, peaking 48
84 hours post infection (**Fig. 1A**). While SARS-CoV-2 titer was slightly lower than that of SARS-
85 CoV at 24 hours post infection, the results were not statistically different. By 48 hours,
86 replication of both viruses had plateaued and significant cytopathic effect (CPE) was observed
87 for both SARS-CoV and SARS-CoV-2 infections. Together, the results indicated that SARS-CoV
88 and SARS-CoV-2 replicate with similar replication kinetics in Vero E6 cells.

89 We next evaluated the susceptibility of SARS-CoV-2 to IFN-I pretreatment. Treatment
90 with IFN-I (recombinant IFN- α) has been attempted as an antiviral approach for a wide variety of
91 pathogens including hepatitis B and C viruses as well as HIV (20). During both the SARS and
92 MERS-CoV outbreaks, IFN-I has been employed with limited effect (21, 22). In this study, we
93 pretreated Vero E6 cells with 1000 U/mL of recombinant IFN-I (IFN- α) 18 hours prior to
94 infection. Vero E6 lack the capacity to produce IFN-I, but are able to respond to exogenous
95 treatment (23). Following pretreatment with IFN-I, SARS-CoV infection has a modest reduction
96 in viral titer of 1.5 log₁₀ plaque forming units (PFU) as compared to untreated control 24 hours
97 post infection (**Fig. 1A**). However, by 48 hours, SARS-CoV has nearly equivalent viral yields as
98 the untreated conditions (7.2 log₁₀PFU versus 7.5 log₁₀PFU). In contrast, SARS-CoV-2 shows a
99 significant reduction in viral replication following IFN-I treatment. At both 24 and 48 hours post
100 infection, SARS-CoV-2 had massive 3-log₁₀ (24 HPI) and 4-log₁₀ (48 HPI) drops in viral titer as

101 compared to control untreated cells. Together, the results demonstrate a clear sensitivity to a
102 primed IFN-I response in SARS-CoV-2, which is not observed with SARS-CoV.

103 To explore differences in IFN-I antagonism between SARS-CoV and SARS-CoV-2, we
104 examined both STAT1 activation and IFN stimulated gene (ISG) expression following IFN-I
105 pretreatment and infection. Examining Vero cell protein lysates, we found that IFN-I treated cells
106 infected with SARS-CoV-2 induced phosphorylated STAT1 by 48 hours post infection (**Fig. 1B**).
107 SARS-CoV had no evidence of STAT1 phosphorylation in either IFN-I treated or untreated cells,
108 illustrating robust control over IFN-I signaling pathways. In contrast, SARS-CoV-2 is unable to
109 control signaling upon IFN-I treatment. Examining further, IFITM1, a known ISG (17), had
110 increased protein expression in the context of SARS-CoV-2 infection following IFN-I
111 pretreatment compared to SARS-CoV under the same conditions (**Fig. 1B**). Basal STAT1 levels
112 are reduced during SARS-CoV infection relative to uninfected control and to a lesser extent
113 during SARS-CoV-2, likely due to the mRNA targeting activity of non-structural protein 1 (NSP1)
114 (24). However, IFN-I treatment results in augmented protein levels for IFITM1 following SARS-
115 CoV-2 infection as compared to untreated SARS-CoV-2. In contrast, IFN-I treated SARS-CoV
116 had no significant increase in IFITM1 relative to control infection. Together, the STAT1
117 phosphorylation, ISG production, and viral protein levels indicate that SARS-CoV-2 lacks the
118 same capacity to modulate the IFN-I stimulated response as the original SARS-CoV.

119 **SARS-CoV-2 attenuated in interferon competent cells.**

120 While capable of responding to exogenous IFN-I, Vero cells lack the capacity to produce
121 IFN-I following infection which likely plays a role in supporting robust replication of a wide range
122 of viruses. To evaluate SARS-CoV-2 in a IFN-I responsive cell type, we infected Calu3 2B4
123 cells, a lung epithelial cell line sorted for ACE2 expression and previously used in coronavirus
124 and influenza research (25). Using an MOI of 1, we examined the viral replication kinetics of
125 SARS-CoV-2 relative to SARS-CoV in Calu3 cells. We found that both SARS-CoV and SARS-

126 CoV-2 replicate with similar overall kinetics, peaking 24 hours post infection (**Fig. 2A**). However,
127 SARS-CoV-2 replication is slightly attenuated relative to SARS-CoV at 24 hours post infection
128 ($0.82 \log_{10}$ reduction). The attenuation in viral replication expands at 48 hours ($1.4 \log_{10}$
129 reduction) indicating a significant change in total viral titers between SARS-CoV and SARS-
130 CoV-2. Notably, no similar attenuation was observed in untreated Vero cells (**Fig. 1A**)
131 suggesting possible immune modulation of SARS-CoV-2 infection in the respiratory cell line,
132 due to differential sensitivity to secreted IFN-I during infection. We next evaluated the
133 susceptibility of SARS-CoV-2 to IFN-I pretreatment in Calu3 cells. When pretreating cells with
134 1000 U/mL of recombinant IFN-I 18 hours prior to infection, SARS-CoV infection has a modest
135 reduction in viral titer of $\sim 0.8 \log_{10}$ PFU as compared to untreated control at both 24 and 48
136 hours post infection (**Fig. 2A**). Similar to Vero cell results, SARS-CoV-2 shows a significant
137 reduction in viral replication following IFN-I treatment in Calu3 cells. At both 24 and 48 hours
138 post infection, SARS-CoV-2 had $2.65 \log_{10}$ (24 HPI) and $2 \log_{10}$ (48 HPI) drops in viral titer,
139 respectively, as compared to control untreated Calu3 cells. Together, the results demonstrate a
140 clear sensitivity to a primed IFN-I response in SARS-CoV-2, which is not observed with SARS-
141 CoV.

142 To further evaluate activation by IFN-I, we examined both STAT1 phosphorylation and
143 ISG expression following infection of Calu3 2B4 cells at 48 hours. Probing cell protein lysates,
144 we found that untreated cells infected with SARS-CoV or SARS-CoV-2 induced phosphorylated
145 STAT1 by 48 hours post infection (**Fig. 2B**). However, the level of STAT1 is markedly
146 diminished in SARS-CoV infection as compared to SARS-CoV-2 suggesting the original
147 epidemic strain disrupts the expression of the ISG. The diminished STAT1 levels in SARS-CoV
148 correspond to robust spike expression in untreated cells. In contrast, SARS-CoV-2 spike is
149 reduced as compared to SARS-CoV, consistent with lower replication observed in untreated
150 Calu3 cells (**Fig. 2A**). The noticeable IFITM1 expression levels observed in untreated Calu3

151 cells infected with SARS-CoV-2 that were not observed in Vero cells may signify higher ISG
152 levels in Calu3 cells during SARS-CoV-2 infection and may contribute to its attenuation relative
153 to SARS-CoV.

154 Following IFN-I pretreatment in Calu3 cells the differences in STAT1 activation and ISG
155 induction are less prominent compared the Vero experiments, likely due to an already induced
156 IFN-I response to the virus infection. However, we still found a reduction in STAT1
157 phosphorylation and ISG induction in IFN-I pretreated SARS-CoV versus SARS-CoV-2
158 infection. Total STAT1 levels were augmented in IFN-I treated cells following SARS-CoV
159 infection to values similar to control IFN-I treated cells. In contrast, SARS-CoV-2 STAT1 levels
160 remained amplified relative to SARS-CoV, but were similar to untreated SARS-CoV-2 infection.
161 Although marginal, IFITM1 expression was slightly increased in IFN-I pretreatment SARS-CoV-
162 2 relative to SARS-CoV. Importantly, the spike protein levels show a significant impact of IFN-I
163 on SARS-CoV infection consistent with titer. For SARS-CoV-2, the spike blot demonstrates the
164 massive attenuation in the presence of IFN-I. Overall, the results in Calu3 cells are consistent
165 with Vero cell findings and indicate a significant sensitivity of SARS-CoV-2 to IFN-I
166 pretreatment.

167 **SARS-CoV-2 blocks IFN-I signaling in polarized human airway epithelial cultures.**

168 Having established IFN-I sensitivity in Vero cells and Calu3 respiratory cell lines, we next sought
169 to evaluate SARS-CoV-2 in polarized human airway epithelial cultures (HAEC). These cultures
170 provide both the complexity of different cell types and the architecture of the human respiratory
171 epithelium. Previous work with SARS-CoV had already established its capacity to control the
172 IFN-I response in human airway cultures (26). Therefore, to examine the impact on overall level
173 of IFN-I signaling in HAECs, we compared SARS-CoV-2 infection to influenza A virus (H1N1)
174 infection, known to induce robust innate immune responses in these cultures. Briefly, HAEC
175 were pretreated with IFN- α on the basolateral side prior to and during infection (**Fig. 3A**). Apical

176 washes were collected at multiple time points and analyzed for viral infectious titers by plaque
177 assay. In addition, culture lysates at endpoint were examined for STAT1 phosphorylation by
178 western blot. Both influenza A and SARS-CoV-2 triggered different levels of immune stimulation
179 (**Fig. 3B**). Influenza A virus infection alone induced robust expression of both total and
180 phosphorylated STAT1 48 hours post infection. In stark contrast, SARS-CoV-2 infection alone
181 indicated no increase in STAT1 or phosphorylated STAT1. IFN-I pretreatment resulted in robust
182 induction of STAT1 and pSTAT1 in all cultures. Despite the distinct immune stimulation profiles
183 upon infection alone, both viruses robustly replicated in the HAEC, with influenza A virus
184 achieving higher viral yields as compared to SARS-CoV-2 (**Fig. 3C & 3D**). Pretreatment
185 reduced influenza infection $\sim 1.5 \log_{10}$ at both 24 and 48 hours post infection, consistent with
186 previous reports (27). In contrast, IFN-I pretreatment nearly ablated SARS-CoV-2 with 2- \log_{10}
187 and 4- \log_{10} reduction in viral titers at 24 and 48 hours relative to untreated controls. Together,
188 the results highlight the capacity of SARS-CoV-2 to prevent IFN-I signaling, but also
189 demonstrate the sensitivity of SARS-CoV-2 to IFN-I pretreatment.

190 **SARS-CoV-2 impacted by IFN-I post treatment.** Having established that SARS-CoV-2 cannot
191 overcome a pre-induced IFN-I state, we next evaluated the impact of IFN-I treatment post
192 infection. Vero cells were infected with SARS-CoV or SARS-CoV-2 at an MOI 0.01 and
193 subsequently treated with 1000 U/mL IFN- α four hours post infection. For SARS-CoV, treatment
194 post infection had no significant impact on viral yields either 24 or 48 hours post infection,
195 consistent with findings from pretreatment experiments. In contrast, SARS-CoV-2 had a
196 substantial 2- \log_{10} reduction in viral titers at 24 hours post infection relative to control. However,
197 by 48 hours, SARS-CoV-2 replication had achieved similar level to untreated controls indicating
198 that post treatment had only a transient impact in Vero cells. We subsequently performed the
199 post-treatment experiment utilizing Calu3 respiratory cells at an MOI 1. Similar to Vero cells,
200 SARS-CoV infection post treatment resulted in no significant changes at 24 hours and has a

201 modest decrease ($\sim 0.5 \log_{10}$) at 48 hours, illustrating its resistance to IFN-I. In contrast, IFN-I
202 post-treatment of SARS-CoV-2 infection resulted in a $>2\text{-log}_{10}$ reduction in viral titers at 24 hours
203 and expanded at 48 hours post ($\sim 4\text{-log}_{10}$ reduction). The results indicate that in Calu3 cells,
204 SARS-CoV-2 is unable to prevent inhibitory effects of IFN-I even after establishing initial
205 infection. Overall, the pre- and post-treatment data highlight distinct differences between
206 SARS-CoV and SARS-CoV-2 in modulation of IFN-I pathways.

207 **Conservation of IFN-I antagonists across SARS-CoV and SARS-CoV-2**

208 Previous work has established several key IFN-I antagonists in the SARS-CoV genome,
209 including NSP1, NSP3, ORF3b, ORF6, and others (28). Considering SARS-CoV-2's sensitivity
210 to IFN-I, we next sought to evaluate conservation of IFN-I antagonist proteins encoded by
211 SARS-CoV-2, SARS-CoV, and several bat SARS-like viruses including WIV16-CoV (29),
212 SHC014-CoV (30), and HKU3.1-CoV (31). Using sequence analysis, we found several changes
213 to SARS-CoV-2 that potentially contribute to IFN-I sensitivity (**Fig. 4**). For SARS-CoV structural
214 proteins, including the nucleocapsid (N) and matrix (M) protein, a high degree of sequence
215 homology ($>90\%$ AA identity) suggests that their reported IFN-I antagonism is likely maintained
216 in SARS-CoV-2 and other SARS-like viruses. Similarly, the ORF1ab poly-protein retains high
217 sequence identity in SARS-CoV-2 and several known IFN-I antagonists contained within the
218 poly-protein (NSP1, NSP7, NSP14-16) are highly conserved relative to SARS-CoV. One notable
219 exception is the large papain-like protease, NSP3, which is only 76% conserved between
220 SARS-CoV and SARS-CoV-2. However, SARS-CoV-2 does maintain a deubiquitinating domain
221 thought to confer IFN-I resistance (32). For SARS-CoV ORF3b, a 154 amino acid (AA) protein
222 known to antagonize IFN-I responses by blocking IRF3 phosphorylation (33), sequence
223 alignment indicates that the SARS-CoV-2 equivalent ORF3b contains a premature stop codon
224 resulting in a truncated 24 AA protein. Similarly, HKU3.1-CoV also has a premature termination
225 resulting in a predicted 39 AA protein. Both WIV16-CoV and SHC014-CoV, the most closely

226 related bat viruses to SARS-CoV, encode longer 114 AA truncated protein with >99% homology
227 with SARS-CoV ORF3b suggesting that IFN-I antagonism might be maintained in these specific
228 group 2B CoV strains. In addition, SARS-CoV ORF6 has been shown to be an IFN-I antagonist
229 that disrupts karyopherin-mediated transportation of transcription factors like STAT1 (33, 34). In
230 contrast to ORF3b, all five surveyed group 2B CoVs maintain ORF6; however, SARS-CoV-2
231 had only 69% homology with SARS-CoV while the other three group 2B bat CoVs had >90%
232 conservation. Importantly, SARS-CoV-2 has a two amino acid truncation in its ORF6; previous
233 work has found that alanine substitution in this C-terminus of SARS-CoV ORF6 resulted in
234 ablated antagonism (34). Together, the sequence homology analysis suggests that differences
235 in NSP3, ORF3b, and/or ORF6 may be key drivers of SARS-CoV-2 IFN-I susceptibility.

236 **Discussion**

237 With the ongoing outbreak of COVID-19 caused by SARS-CoV-2, viral characterization remains
238 a key factor in responding to the emergent novel virus. In this report, we describe differences in
239 the IFN-I sensitivity between SARS-CoV-2 and the original SARS-CoV. While both viruses
240 maintain similar replication in untreated Vero E6 cells, SARS-CoV-2 has a significant decrease
241 in viral protein and replication following IFN-I pretreatment. The decreased SARS-CoV-2
242 replication correlates with phosphorylation of STAT1 and augmented ISG expression largely
243 absent following SARS-CoV infection despite IFN-I pretreatment. Infection of IFN-I competent
244 Calu3 2B4 cells resulted in reduced SARS-CoV-2 replication relative to SARS-CoV; IFN-I
245 pretreatment also corresponded to increased sensitivity for SARS-CoV-2 in Calu3 cells.
246 However, SARS-CoV-2 fails to induce IFN-I pathways during infection of unprimed polarized
247 HAEC as compared to influenza A virus, suggesting a capacity to control IFN-I signaling. Yet,
248 pretreatment nearly ablates replication of SARS-CoV-2 highlighting robust sensitivity to IFN-I
249 pathways once activated. Finally, SARS-CoV-2, unlike SARS-CoV, responded to post-infection
250 IFN-I treatment with reduced viral yields in both Vero and Calu3 cells. Analysis of viral proteins

251 finds SARS-CoV-2 has several changes that potentially impact its capacity to modulate the IFN-
252 I response, including loss of an equivalent ORF3b and a short truncation of ORF6, both known
253 as IFN-I antagonists for SARS-CoV (33). Together, our results suggest SARS-CoV and SARS-
254 CoV-2 have differences in their ability to antagonize the IFN-I response once initiated and that
255 this may have major implications for COVID-19 disease and treatment.

256 With a similar genome organization and disease symptoms in humans, the SARS-CoV-2
257 outbreak has drawn insights from the closely related SARS-CoV. However, the differences in
258 sensitivity to IFN-I pretreatment illustrate a clear distinction between the two CoVs. Coupled with
259 a novel furin cleavage site (35), robust upper airway infection (8), and transmission prior to
260 symptomatic disease (36), the differences between SARS-CoV and SARS-CoV-2 could prove
261 important in disrupting the ongoing spread of COVID-19. For SARS-CoV, *in vitro* studies have
262 consistently found that wild-type SARS-CoV is indifferent to IFN-I pretreatment (37, 38).
263 Similarly, *in vivo* SARS-CoV studies have found that the loss of IFN-I signaling had no
264 significant impact on disease (39), suggesting that this virus is not sensitive to the antiviral
265 effects of IFN-I. However, more recent reports suggest that host genetic background may
266 majorly influence this finding (40). For SARS-CoV-2, our results suggest that IFN-I pretreatment
267 produces a 3 - 4 log₁₀ drop in viral titer. This level of sensitivity is similar to MERS-CoV and
268 suggests that the novel CoV lacks the same capacity to escape a primed IFN-I response as
269 SARS-CoV (41, 42). Notably, the sensitivity to IFN-I does not completely ablate viral replication;
270 unlike SARS-CoV 2' O methyl-transferase mutants (37), SARS-CoV-2 is able to replicate to low,
271 detectable levels even in the presence of IFN-I. This finding could help explain positive test
272 results in patients with minimal symptoms and the range of disease observed. In addition, while
273 SARS-CoV-2 is sensitive to IFN-I pretreatment, both SARS-CoV and MERS-CoV employ
274 effective means to disrupt virus recognition and downstream signaling until late during infection
275 (25). While SARS-CoV-2 may employ a similar mechanism early during infection, STAT1

276 phosphorylation and reduced viral replication are observed in IFN-I primed and post-treatment
277 conditions indicating that the novel CoV does not block IFN-I signaling as effectively as the
278 original SARS-CoV.

279 For SARS-CoV-2, the sensitivity to IFN-I indicates a distinction from SARS-CoV and
280 suggests differential host innate immune modulation between the viruses. The distinct ORF3b
281 and truncation/changes in ORF6 could signal a reduced capacity of SARS-CoV-2 to interfere
282 with IFN-I responses. For SARS-CoV ORF6, the N-terminal domain has been shown to have a
283 clear role in its ability to disrupt karyopherin-mediated STAT1 transport (34); in turn, the loss or
284 reduction of ORF6 function for SARS-CoV-2 would likely render it much more susceptible to
285 IFN-I pretreatment as activated STAT1 has the capacity to enter the nucleus and induce ISGs
286 and the antiviral response. In these studies, we have found that following IFN-I pretreatment,
287 STAT1 phosphorylation is induced following SARS-CoV-2 infection. The increase in ISG
288 proteins (STAT1, IFITM1) suggests that SARS-CoV-2 ORF6 does not effectively block nuclear
289 transport as well as SARS-CoV ORF6. For SARS-CoV ORF3b, the viral protein has been
290 shown to disrupt phosphorylation of IRF3, a key transcriptional factor in the production of IFN-I
291 and the antiviral state (33). While its mechanism of action is not clear, the ORF3b absence in
292 SARS-CoV-2 infection likely impacts its ability to inhibit the IFN-I response and eventual STAT1
293 activation. Similarly, while NSP3 deubiquitinating domain remains intact, SARS-CoV-2 has a 24
294 AA insertion upstream of this deubiquitinating domain that could potentially alter that function
295 (32). While other antagonists are maintained with high levels of conservation (>90%), single
296 point mutations in key locations could modify function and contribute to increased IFN-I
297 sensitivity. Overall, the sequence analysis suggests that differences between SARS-CoV and
298 SARS-CoV-2 viral proteins may drive attenuation in the context of IFN-I pretreatment.

299 The increased sensitivity of SARS-CoV-2 suggests utility in treatment using IFN-I. While
300 IFN-I has been used in response to chronic viral infection (43), previous examination of SARS-

301 CoV cases found inconclusive effect for IFN-I treatment (44). However, the findings from the
302 SARS-CoV outbreak were complicated by combination therapy of IFN-I with other treatments
303 including ribavirin/steroids and lack of a regimented protocol. While IFN-I has been utilized to
304 treat MERS-CoV infected patients, no conclusive data yet exists to determine efficacy (45). Yet,
305 *in vivo* studies with MERS-CoV have found that early induction with IFN-I can be protective in
306 mice (46); importantly, the same study found that late IFN-I activation can be detrimental for
307 MERS-CoV disease (46). Similarly, early reports have described treatments using IFN-I in
308 combination for SARS-CoV-2 infection; yet the efficacy of these treatments and the parameters
309 of their use are not known (47). Overall, sensitivity data suggest that IFN-I treatment may have
310 utility for treating SARS-CoV-2 if the appropriate parameters can be determined. In addition, use
311 of type III IFN, which is predicted to have utility in the respiratory tract, could offer another
312 means for effective treatment for SARS-CoV-2.

313 In addition to treatment, the sensitivity to IFN-I may also have implications for animal
314 model development. For SARS-CoV, mouse models that recapitulate human disease were
315 developed through virus passage in immune competent mice (48). Similarly, mouse models for
316 MERS-CoV required adaptation in mice that had genetic modifications of their dipeptidyl-
317 peptidase 4 (DPP4), the receptor for MERS-CoV (49, 50). However, each of these MERS-CoV
318 mouse models still retained full immune capacity. In contrast, SARS-CoV-2 sensitivity to IFN-I
319 may signal the need to use an immune deficient model to develop relevant disease. While initial
320 work has suggested incompatibility to SARS-CoV-2 infection in mice based on receptor usage
321 (8), the IFN-I response may be a second major barrier that needs to be overcome. Similar to
322 the emergent Zika virus outbreak, the use of IFN-I receptor knockout mice or IFN-I receptor
323 blocking antibody may be necessary to develop a useful SARS-CoV-2 animal models for
324 therapeutic testing (51).

325 Overall, our results indicate that SARS-CoV-2 has a much higher sensitivity to type I IFN
326 than the previously emergent SARS-CoV. This augmented type I IFN sensitivity is likely due to
327 changes in viral proteins between the two epidemic CoV strains. Moving forward, these data
328 could provide important insights for both the treatment of SARS-CoV-2 as well as developing
329 novel animal models of disease. In this ongoing outbreak, the results also highlight a distinction
330 between the highly related viruses and suggest insights from SARS-CoV must be verified for
331 SARS-CoV-2 infection and disease.

332

333 **Methods**

334 **Viruses and cells.** SARS-CoV-2 USA-WA1/2020 was provided by the World Reference Center
335 for Emerging Viruses and Arboviruses (WRCEVA) or BEI Resources and was originally
336 obtained from the USA Centers of Disease Control as described (52). SARS-CoV-2 and mouse-
337 adapted recombinant SARS-CoV (MA15) (48) were titrated and propagated on Vero E6 cells,
338 grown in DMEM with 5% fetal bovine serum and 1% antibiotic/antimycotic (Gibco). Calu3 2B4
339 cells were grown in DMEM with 10% defined fetal bovine serum, 1% sodium pyruvate (Gibco),
340 and 1% antibiotic/antimycotic (Gibco). Standard plaque assays were used for SARS-CoV and
341 SARS-CoV-2 (26, 53). All experiments involving infectious virus were conducted at the
342 University of Texas Medical Branch (Galveston, TX) or New York University School of Medicine
343 (New York City, NY) in approved biosafety level 3 (BSL) laboratories with routine medical
344 monitoring of staff.

345 **Infection and type I IFN pre- and post-treatment.** Viral replication studies in Vero E6 and
346 Calu3 2B4 cells were performed as previously described (37, 54). Briefly, cells were washed two
347 times with PBS and inoculated with SARS-CoV or SARS-CoV-2 at a multiplicity of infection
348 (MOI) 0.01 for 60 minutes at 37 °C. Following inoculation, cells were washed 3 times, and fresh
349 media was added to signify time 0. Three or more biological replicates were harvested at each
350 described time. No blinding was used in any sample collections, nor were samples randomized.
351 For type I IFN pretreatment, experiments were completed as previously described (37). Briefly,
352 Vero E6 cells were incubated with 1000 U/mL of recombinant type I IFN- α (PBL Assay
353 Sciences) 18 hours prior to infection (37). Cells were infected as described above and type I IFN
354 was not added back after infection.

355 **Generation of polarized human airway epithelial cultures (HAEC).**

356 hTert-immortalized human normal airway tracheobronchial epithelial cells, BCI.NS1.1 (55) were
357 maintained in ExPlus growth media (StemCell). To generate HAEC, BCI.NS1.1 were plated
358 (7.5E4 cells/well) on rat-tail collagen type 1-coated permeable transwell membrane supports
359 (6.5mm; Corning Inc), immersed in ExPlus growth media in both the apical and basal chamber.
360 Upon reaching confluency, media in the apical chamber was removed (airlift), and media in the
361 basal chamber was changed to Pneumacult ALI maintenance media (StemCell). Pneumacult
362 ALI maintenance media was changed every two days for approximately 6 weeks to form
363 differentiated, polarized cultures that resemble in vivo pseudostratified mucociliary epithelium.

364 **IFN-I treatment and infection of HAEC.**

365 For interferon pretreatment of human airway epithelial cultures, 1000 U/mL of universal
366 recombinant interferon-alpha was added to the basolateral chamber 2 h prior to viral infections.
367 For viral infections, cultures were washed apically with 50 µl of prewarmed PBS three times for
368 30 min at 37°C. Virus inoculates (1.3E6 PFU for influenza A/California/07/2009 (H1N1) virus
369 and 1.35E5 PFU for SARS-CoV-2 USA/WA/1/2020 in 50 µl PBS Mg/Ca) were added apically for
370 two hours. Inoculates were then removed and cultures were washed three times with PBS, the
371 third wash was collected and then the cultures were incubated for the indicated times. Progeny
372 virus was collected in apical washes with 50 µl PBS Mg/Ca for 30 min at 8, 24 and 48 hpi
373 (endpoint). At endpoint, the membranes were collected and lysed in 300 µl LDS lysis buffer (Life
374 Technologies). Protein levels were measured by western blot. Briefly, 5 µl of cell lysates were
375 loaded into a SDS-PAGE gel and transferred to a nitrocellulose membrane. The membranes
376 were blocked for 1 h at room temperature with 5% skim milk and then incubated overnight at
377 4°C with appropriate primary antibody dilution: anti-STAT1 (1:1000, Cell Signaling), anti-
378 pSTAT1 (1:1000, Cell Signaling) or anti-beta actin (1:5000, Invitrogen). Then, the membranes
379 were incubated with the recommended dilution of HRP-conjugated secondary antibody (goat
380 anti-rabbit IgG HRP 1:10000, Invitrogen; goat anti-mouse IgG HRP 1:10000, Invitrogen) at room

381 temperature for 1 h. Super Signal West Dura Kit (Thermo Scientific) was used for signal
382 development according to manufacturer's recommendations and the chemiluminescence was
383 detected with a ChemiDoc Imager (BioRad).

384 **Phylogenetic Tree and Sequence Identity Heat Map.** Heat maps were constructed from a set
385 of representative group 2B coronaviruses by using alignment data paired with neighbor-joining
386 phylogenetic trees built in Geneious (v.9.1.5). Sequence identity was visualized using EvolView
387 (<http://evolgenius.info/>) and utilized SARS-CoV Urbani as the reference sequence. Tree shows
388 the degree of genetic similarity of SARS-CoV-2 and SARS-CoV across selected group 2B
389 coronaviruses.

390 **Immunoblot Analysis and Antibodies:**

391 Viral and host protein analysis were evaluated as previously described (52, 56). Briefly, cell
392 lysates were resolved on 7.5% Mini-PROTEAN TGX SDS-PAGE gels and then transferred to
393 polyvinylidene difluoride (PVDF) membranes using a Trans-Blot Turbo transfer system (Bio-
394 Rad). Membranes were blocked with 5% (w/v) non-fat dry milk in TBST (TBS with 0.1% (v/v)
395 Tween-20) for 1 hr, and then probed with the indicated primary antibody in 3% (w/v) BSA in
396 TBST at 4°C overnight. Following overnight incubation, membranes were probed with the
397 following secondary antibodies in 5% (w/v) non-fat dry milk in TBST for 1 hr at room
398 temperature: anti-rabbit or anti-mouse IgG-HRP conjugated antibody from sheep (both 1:10,000
399 GE Healthcare). Proteins were visualized using ECL or SuperSignal West Femto
400 chemiluminescence reagents (Pierce) and detected by autoradiography. The following primary
401 antibodies were used: anti-pSTAT1 (Y701) (1:1000 9171L Cell Signaling Technologies), anti-
402 STAT1 D1K9Y (1:1000 14994P Cell Signaling Technologies), anti-IFITM1 (1:1000 PA5-20989
403 Invitrogen), anti-SARS-CoV/CoV-2 Spike 1A9 (1:1000 GTX632604 GeneTex), and anti- β -Actin
404 (1:1000 ab8227 Abcam).

405 **Statistical analysis.** All statistical comparisons in this manuscript involved the comparison
406 between 2 groups, SARS-CoV or SARS-CoV-2 infected groups under equivalent conditions.
407 Thus, significant differences in viral titer were determined by the unpaired two-tailed student's T-
408 Test.

409 **Acknowledgements.** Research was supported by grants from NIA and NIAID of the NIH
410 (U19AI100625 and R00AG049092 to VDM; R24AI120942 to WRCEVA; R01AI134907 to RR;
411 1R01AI143639-01 and 1R21AI139374-01 to MD; Jan Vilcek/David Goldfarb Fellowship
412 Endowment Funds to AMVJ; and T32 AI007526 to AH). Research was also supported by
413 STARs Award provided by the University of Texas System to VDM and trainee funding provided
414 by the McLaughlin Fellowship Fund at UTMB.

415

416 **References**

- 417 1. **Gralinski LE, Menachery VD.** 2020. Return of the Coronavirus: 2019-nCoV. *Viruses* **12**.
418 2. **Gorbalenya AE, Baker SC, Baric RS, de Groot RJ, Drosten C, Gulyaeva AA,**
419 **Haagmans BL, Lauber C, Leontovich AM, Neuman BW, Penzar D, Perlman S, Poon LLM,**
420 **Samborskiy DV, Sidorov IA, Sola I, Ziebuhr J, Coronaviridae Study Group of the**
421 **International Committee on Taxonomy of V.** 2020. The species Severe acute respiratory
422 syndrome-related coronavirus: classifying 2019-nCoV and naming it SARS-CoV-2. *Nature*
423 *Microbiology* doi:10.1038/s41564-020-0695-z.
424 3. **Zhu N, Zhang D, Wang W, Li X, Yang B, Song J, Zhao X, Huang B, Shi W, Lu R, Niu**
425 **P, Zhan F, Ma X, Wang D, Xu W, Wu G, Gao GF, Tan W, China Novel Coronavirus I,**
426 **Research T.** 2020. A Novel Coronavirus from Patients with Pneumonia in China, 2019. *N Engl J*
427 *Med* **382**:727-733.
428 4. **Huang C, Wang Y, Li X, Ren L, Zhao J, Hu Y, Zhang L, Fan G, Xu J, Gu X, Cheng Z,**
429 **Yu T, Xia J, Wei Y, Wu W, Xie X, Yin W, Li H, Liu M, Xiao Y, Gao H, Guo L, Xie J, Wang G,**
430 **Jiang R, Gao Z, Jin Q, Wang J, Cao B.** 2020. Clinical features of patients infected with 2019
431 novel coronavirus in Wuhan, China. *Lancet* **395**:497-506.
432 5. **Wu Z, McGoogan JM.** 2020. Characteristics of and Important Lessons From the
433 Coronavirus Disease 2019 (COVID-19) Outbreak in China: Summary of a Report of 72314
434 Cases From the Chinese Center for Disease Control and Prevention. *JAMA*
435 doi:10.1001/jama.2020.2648.
436 6. **Xu X, Chen P, Wang J, Feng J, Zhou H, Li X, Zhong W, Hao P.** 2020. Evolution of the
437 novel coronavirus from the ongoing Wuhan outbreak and modeling of its spike protein for risk of
438 human transmission. *Sci China Life Sci* **63**:457-460.
439 7. **Letko M, Marzi A, Munster V.** 2020. Functional assessment of cell entry and receptor
440 usage for SARS-CoV-2 and other lineage B betacoronaviruses. *Nat Microbiol*
441 doi:10.1038/s41564-020-0688-y.
442 8. **Zhou P, Yang XL, Wang XG, Hu B, Zhang L, Zhang W, Si HR, Zhu Y, Li B, Huang**
443 **CL, Chen HD, Chen J, Luo Y, Guo H, Jiang RD, Liu MQ, Chen Y, Shen XR, Wang X, Zheng**
444 **XS, Zhao K, Chen QJ, Deng F, Liu LL, Yan B, Zhan FX, Wang YY, Xiao GF, Shi ZL.** 2020. A
445 pneumonia outbreak associated with a new coronavirus of probable bat origin. *Nature*
446 doi:10.1038/s41586-020-2012-7.
447 9. **de Wit E, Feldmann F, Cronin J, Jordan R, Okumura A, Thomas T, Scott D, Cihlar**
448 **T, Feldmann H.** 2020. Prophylactic and therapeutic remdesivir (GS-5734) treatment in the
449 rhesus macaque model of MERS-CoV infection. *Proc Natl Acad Sci U S A*
450 doi:10.1073/pnas.1922083117.
451 10. **Wang M, Cao R, Zhang L, Yang X, Liu J, Xu M, Shi Z, Hu Z, Zhong W, Xiao G.** 2020.
452 Remdesivir and chloroquine effectively inhibit the recently emerged novel coronavirus (2019-
453 nCoV) in vitro. *Cell Res* doi:10.1038/s41422-020-0282-0.
454 11. **Sheahan TP, Sims AC, Leist SR, Schafer A, Won J, Brown AJ, Montgomery SA,**
455 **Hogg A, Babusis D, Clarke MO, Spahn JE, Bauer L, Sellers S, Porter D, Feng JY, Cihlar T,**
456 **Jordan R, Denison MR, Baric RS.** 2020. Comparative therapeutic efficacy of remdesivir and
457 combination lopinavir, ritonavir, and interferon beta against MERS-CoV. *Nat Commun* **11**:222.
458 12. **Sheahan TP, Sims AC, Graham RL, Menachery VD, Gralinski LE, Case JB, Leist**
459 **SR, Pyrc K, Feng JY, Trantcheva I, Bannister R, Park Y, Babusis D, Clarke MO, Mackman**
460 **RL, Spahn JE, Palmiotti CA, Siegel D, Ray AS, Cihlar T, Jordan R, Denison MR, Baric RS.**
461 2017. Broad-spectrum antiviral GS-5734 inhibits both epidemic and zoonotic coronaviruses. *Sci*
462 *Transl Med* **9**.
463 13. **Ahmed SF, Quadeer AA, McKay MR.** 2020. Preliminary Identification of Potential
464 Vaccine Targets for the COVID-19 Coronavirus (SARS-CoV-2) Based on SARS-CoV
465 Immunological Studies. *Viruses* **12**.

- 466 14. **Medzhitov R, Janeway CA, Jr.** 1997. Innate immunity: the virtues of a nonclonal
467 system of recognition. *Cell* **91**:295-298.
- 468 15. **Meylan E, Tschopp J.** 2006. Toll-like receptors and RNA helicases: two parallel ways to
469 trigger antiviral responses. *Mol Cell* **22**:561-569.
- 470 16. **Akira S.** 2006. TLR signaling. *Curr Top Microbiol Immunol* **311**:1-16.
- 471 17. **Schoggins JW, Wilson SJ, Panis M, Murphy MY, Jones CT, Bieniasz P, Rice CM.**
472 2011. A diverse range of gene products are effectors of the type I interferon antiviral response.
473 *Nature* **472**:481-485.
- 474 18. **Platanias LC.** 2005. Mechanisms of type-I- and type-II-interferon-mediated signalling.
475 *Nat Rev Immunol* **5**:375-386.
- 476 19. **Rajsbaum R, Garcia-Sastre A.** 2013. Viral evasion mechanisms of early antiviral
477 responses involving regulation of ubiquitin pathways. *Trends Microbiol* **21**:421-429.
- 478 20. **Lin FC, Young HA.** 2014. Interferons: Success in anti-viral immunotherapy. *Cytokine*
479 *Growth Factor Rev* **25**:369-376.
- 480 21. **Zumla A, Hui DS, Perlman S.** 2015. Middle East respiratory syndrome. *Lancet*
481 **386**:995-1007.
- 482 22. **Song Z, Xu Y, Bao L, Zhang L, Yu P, Qu Y, Zhu H, Zhao W, Han Y, Qin C.** 2019.
483 From SARS to MERS, Thrusting Coronaviruses into the Spotlight. *Viruses* **11**.
- 484 23. **Diaz MO, Ziemins S, Le Beau MM, Pitha P, Smith SD, Chilcote RR, Rowley JD.** 1988.
485 Homozygous deletion of the alpha- and beta 1-interferon genes in human leukemia and derived
486 cell lines. *Proc Natl Acad Sci U S A* **85**:5259-5263.
- 487 24. **Narayanan K, Ramirez SI, Lokugamage KG, Makino S.** 2015. Coronavirus
488 nonstructural protein 1: Common and distinct functions in the regulation of host and viral gene
489 expression. *Virus Res* **202**:89-100.
- 490 25. **Menachery VD, Eisfeld AJ, Schafer A, Josset L, Sims AC, Proll S, Fan S, Li C,**
491 **Neumann G, Tilton SC, Chang J, Gralinski LE, Long C, Green R, Williams CM, Weiss J,**
492 **Matzke MM, Webb-Robertson BJ, Schepmoes AA, Shukla AK, Metz TO, Smith RD, Waters**
493 **KM, Katze MG, Kawaoka Y, Baric RS.** 2014. Pathogenic influenza viruses and coronaviruses
494 utilize similar and contrasting approaches to control interferon-stimulated gene responses. *MBio*
495 **5**:e01174-01114.
- 496 26. **Sims AC, Tilton SC, Menachery VD, Gralinski LE, Schäfer A, Matzke MM, Webb-**
497 **Robertson BJ, Chang J, Luna ML, Long CE, Shukla AK, Bankhead AR, Burkett SE,**
498 **Zornetzer G, Tseng CT, Metz TO, Pickles R, McWeeney S, Smith RD, Katze MG, Waters**
499 **KM, Baric RS.** 2013. Release of severe acute respiratory syndrome coronavirus nuclear import
500 block enhances host transcription in human lung cells. *J Virol* **87**:3885-3902.
- 501 27. **Österlund P, Pirhonen J, Ikonen N, Rönkkö E, Strengell M, Mäkelä SM, Broman M,**
502 **Hamming OJ, Hartmann R, Ziegler T, Julkunen I.** 2010. Pandemic H1N1 2009 Influenza A
503 Virus Induces Weak Cytokine Responses in Human Macrophages and Dendritic Cells and Is
504 Highly Sensitive to the Antiviral Actions of Interferons. *Journal of Virology* **84**:1414-1422.
- 505 28. **Totura AL, Baric RS.** 2012. SARS coronavirus pathogenesis: host innate immune
506 responses and viral antagonism of interferon. *Curr Opin Virol* **2**:264-275.
- 507 29. **Yang XL, Hu B, Wang B, Wang MN, Zhang Q, Zhang W, Wu LJ, Ge XY, Zhang YZ,**
508 **Daszak P, Wang LF, Shi ZL.** 2015. Isolation and Characterization of a Novel Bat Coronavirus
509 Closely Related to the Direct Progenitor of Severe Acute Respiratory Syndrome Coronavirus. *J*
510 *Virol* **90**:3253-3256.
- 511 30. **Ge XY, Li JL, Yang XL, Chmura AA, Zhu G, Epstein JH, Mazet JK, Hu B, Zhang W,**
512 **Peng C, Zhang YJ, Luo CM, Tan B, Wang N, Zhu Y, Crameri G, Zhang SY, Wang LF,**
513 **Daszak P, Shi ZL.** 2013. Isolation and characterization of a bat SARS-like coronavirus that
514 uses the ACE2 receptor. *Nature* **503**:535-538.

- 515 31. **Lau SK, Woo PC, Li KS, Huang Y, Tsoi HW, Wong BH, Wong SS, Leung SY, Chan**
516 **KH, Yuen KY.** 2005. Severe acute respiratory syndrome coronavirus-like virus in Chinese
517 horseshoe bats. *Proc Natl Acad Sci U S A* **102**:14040-14045.
- 518 32. **Clementz MA, Chen Z, Banach BS, Wang Y, Sun L, Ratia K, Baez-Santos YM, Wang**
519 **J, Takayama J, Ghosh AK, Li K, Mesecar AD, Baker SC.** 2010. Deubiquitinating and
520 interferon antagonism activities of coronavirus papain-like proteases. *J Virol* **84**:4619-4629.
- 521 33. **Kopecky-Bromberg SA, Martinez-Sobrido L, Frieman M, Baric RA, Palese P.** 2007.
522 Severe acute respiratory syndrome coronavirus open reading frame (ORF) 3b, ORF 6, and
523 nucleocapsid proteins function as interferon antagonists. *J Virol* **81**:548-557.
- 524 34. **Frieman M, Yount B, Heise M, Kopecky-Bromberg SA, Palese P, Baric RS.** 2007.
525 Severe acute respiratory syndrome coronavirus ORF6 antagonizes STAT1 function by
526 sequestering nuclear import factors on the rough endoplasmic reticulum/Golgi membrane. *J*
527 *Virol* **81**:9812-9824.
- 528 35. **Coutard B, Valle C, de Lamballerie X, Canard B, Seidah NG, Decroly E.** 2020. The
529 spike glycoprotein of the new coronavirus 2019-nCoV contains a furin-like cleavage site absent
530 in CoV of the same clade. *Antiviral Res* **176**:104742.
- 531 36. **Tong ZD, Tang A, Li KF, Li P, Wang HL, Yi JP, Zhang YL, Yan JB.** 2020. Potential
532 Presymptomatic Transmission of SARS-CoV-2, Zhejiang Province, China, 2020. *Emerg Infect*
533 *Dis* **26**.
- 534 37. **Menachery VD, Yount BL, Jr., Josset L, Gralinski LE, Scobey T, Agnihothram S,**
535 **Katze MG, Baric RS.** 2014. Attenuation and restoration of severe acute respiratory syndrome
536 coronavirus mutant lacking 2'-o-methyltransferase activity. *J Virol* **88**:4251-4264.
- 537 38. **Thiel V, Weber F.** 2008. Interferon and cytokine responses to SARS-coronavirus
538 infection. *Cytokine Growth Factor Rev* **19**:121-132.
- 539 39. **Frieman MB, Chen J, Morrison TE, Whitmore A, Funkhouser W, Ward JM,**
540 **Lamirande EW, Roberts A, Heise M, Subbarao K, Baric RS.** 2010. SARS-CoV pathogenesis
541 is regulated by a STAT1 dependent but a type I, II and III interferon receptor independent
542 mechanism. *PLoS Pathog* **6**:e1000849.
- 543 40. **Channappanavar R, Fehr AR, Vijay R, Mack M, Zhao J, Meyerholz DK, Perlman S.**
544 2016. Dysregulated Type I Interferon and Inflammatory Monocyte-Macrophage Responses
545 Cause Lethal Pneumonia in SARS-CoV-Infected Mice. *Cell Host Microbe* **19**:181-193.
- 546 41. **Menachery VD, Gralinski LE, Mitchell HD, Dinnon KH, 3rd, Leist SR, Yount BL, Jr.,**
547 **Graham RL, McAnarney ET, Stratton KG, Cockrell AS, Debbink K, Sims AC, Waters KM,**
548 **Baric RS.** 2017. Middle East Respiratory Syndrome Coronavirus Nonstructural Protein 16 Is
549 Necessary for Interferon Resistance and Viral Pathogenesis. *mSphere* **2**.
- 550 42. **Falzarano D, de Wit E, Martellaro C, Callison J, Munster VJ, Feldmann H.** 2013.
551 Inhibition of novel beta coronavirus replication by a combination of interferon-alpha2b and
552 ribavirin. *Sci Rep* **3**:1686.
- 553 43. **Finter NB, Chapman S, Dowd P, Johnston JM, Manna V, Sarantis N, Sheron N,**
554 **Scott G, Phua S, Tatum PB.** 1991. The use of interferon-alpha in virus infections. *Drugs*
555 **42**:749-765.
- 556 44. **Stockman LJ, Bellamy R, Garner P.** 2006. SARS: systematic review of treatment
557 effects. *PLoS Med* **3**:e343.
- 558 45. **de Wit E, van Doremalen N, Falzarano D, Munster VJ.** 2016. SARS and MERS:
559 recent insights into emerging coronaviruses. *Nat Rev Microbiol* **14**:523-534.
- 560 46. **Channappanavar R, Fehr AR, Zheng J, Wohlford-Lenane C, Abrahante JE, Mack M,**
561 **Sompallae R, McCray PB, Jr., Meyerholz DK, Perlman S.** 2019. IFN-I response timing
562 relative to virus replication determines MERS coronavirus infection outcomes. *J Clin Invest*
563 **130**:3625-3639.
- 564 47. **Pang J, Wang MX, Ang IYH, Tan SHX, Lewis RF, Chen JI, Gutierrez RA, Gwee**
565 **SXW, Chua PEY, Yang Q, Ng XY, Yap RK, Tan HY, Teo YY, Tan CC, Cook AR, Yap JC, Hsu**

- 566 **LY.** 2020. Potential Rapid Diagnostics, Vaccine and Therapeutics for 2019 Novel Coronavirus
567 (2019-nCoV): A Systematic Review. *J Clin Med* **9**.
- 568 48. **Roberts A, Deming D, Paddock CD, Cheng A, Yount B, Vogel L, Herman BD,**
569 **Sheahan T, Heise M, Genrich GL, Zaki SR, Baric R, Subbarao K.** 2007. A mouse-adapted
570 SARS-coronavirus causes disease and mortality in BALB/c mice. *PLoS Pathog* **3**:e5.
- 571 49. **Cockrell A YB, Scobey T, Jensen K, Douglas M, Beall A, Tang X-C, Marasco WA,**
572 **Heise MT, Baric RS** 2016. A Mouse Model for MERS Coronavirus Induced Acute Respiratory
573 Distress Syndrome. *Nature Microbiology* **In Press**.
- 574 50. **Li K, Wohlford-Lenane CL, Channappanavar R, Park JE, Earnest JT, Bair TB, Bates**
575 **AM, Brogden KA, Flaherty HA, Gallagher T, Meyerholz DK, Perlman S, McCray PB, Jr.**
576 2017. Mouse-adapted MERS coronavirus causes lethal lung disease in human DPP4 knockin
577 mice. *Proc Natl Acad Sci U S A* **114**:E3119-E3128.
- 578 51. **Lazear HM, Govero J, Smith AM, Platt DJ, Fernandez E, Miner JJ, Diamond MS.**
579 2016. A Mouse Model of Zika Virus Pathogenesis. *Cell Host Microbe* **19**:720-730.
- 580 52. **Harcourt J, Tamin A, Lu X, Kamili S, Sakthivel SK, Murray J, Queen K, Tao Y,**
581 **Paden CR, Zhang J, Li Y, Uehara A, Wang H, Goldsmith C, Bullock HA, Wang L, Whitaker**
582 **B, Lynch B, Gautam R, Schindewolf C, Lokugamage KG, Scharton D, Plante JA,**
583 **Mirchandani D, Widen SG, Narayanan K, Makino S, Ksiazek TG, Plante KS, Weaver SC,**
584 **Lindstrom S, Tong S, Menachery VD, Thornburg NJ.** 2020. Severe Acute Respiratory
585 Syndrome Coronavirus 2 from Patient with 2019 Novel Coronavirus Disease, United States.
586 *Emerg Infect Dis* **26**.
- 587 53. **Josset L, Menachery VD, Gralinski LE, Agnihothram S, Sova P, Carter VS, Yount**
588 **BL, Graham RL, Baric RS, Katze MG.** 2013. Cell host response to infection with novel human
589 coronavirus EMC predicts potential antivirals and important differences with SARS coronavirus.
590 *MBio* **4**:e00165-00113.
- 591 54. **Sheahan T, Rockx B, Donaldson E, Corti D, Baric R.** 2008. Pathways of cross-
592 species transmission of synthetically reconstructed zoonotic severe acute respiratory syndrome
593 coronavirus. *J Virol* **82**:8721-8732.
- 594 55. **Walters MS, Gomi K, Ashbridge B, Moore MA, Arbelaez V, Heldrich J, Ding BS,**
595 **Rafii S, Staudt MR, Crystal RG.** 2013. Generation of a human airway epithelium derived basal
596 cell line with multipotent differentiation capacity. *Respir Res* **14**:135.
- 597 56. **van Tol S, Atkins C, Bharaj P, Johnson KN, Hage A, Freiberg AN, Rajsbaum R.**
598 2020. VAMP8 Contributes to the TRIM6-Mediated Type I Interferon Antiviral Response during
599 West Nile Virus Infection. *J Virol* **94**.

600

601

602 **Figure Legends**

603 **Figure 1. SARS-CoV-2 sensitive to type I IFN pretreatment.** A) Vero E6 cells were treated
604 with 1000 U/mL recombinant type I (hashed line) IFN or mock (solid line) for 18 hours prior to
605 infection. Cells were subsequently infected with either SARS-CoV WT (black) or SARS-CoV-2
606 (blue) at an MOI of 0.01 as described above. Each point on the line graph represents the group
607 mean, $N \geq 3$. All error bars represent SD. The two tailed students t-test was used to determine
608 P-values: *** $P < 0.001$. B) Vero cell protein lysates from IFN-I treated and untreated cells were
609 probed 48 hours post infection by Western blotting for phosphorylated STAT1 (Y701), STAT1,
610 IFITM1, SARS spike, and Actin.

611 **Figure 2. SARS-CoV-2 attenuated and IFN-I sensitive in Calu3 respiratory cells.** A) Calu3
612 2B4 cells were treated with 1000 U/mL recombinant type I (hashed line) IFN or mock (solid line)
613 for 18 hours prior to infection. Cells were subsequently infected with either SARS-CoV WT
614 (black) or SARS-CoV-2 (blue) at an MOI of 1. Each point on the line graph represents the
615 group mean, $N \geq 3$. All error bars represent SD. The two tailed students t-test was used to
616 determine P-values: *** $P < 0.001$. B) Calu3 cell protein lysates from IFN-I treated and untreated
617 cells were probed 48 hours post infection by Western blotting for phosphorylated STAT1 (Y701),
618 STAT1, IFITM1, SARS spike, and Actin.

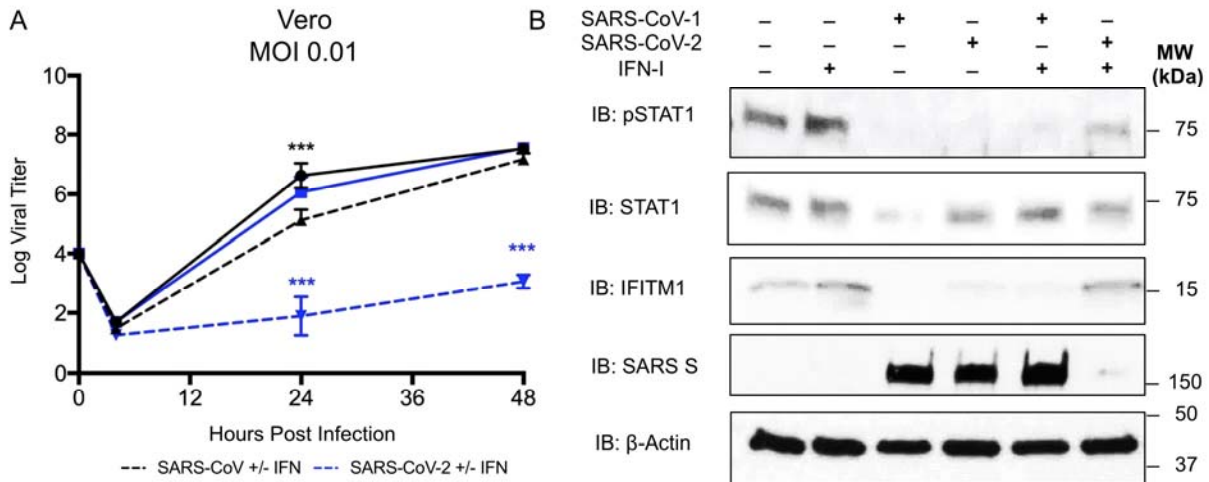
619 **Figure 3. Differential IFN-I sensitivity and pSTAT1 phosphorylation following SARS-CoV-**
620 **2 or influenza A virus on polarized human airway epithelial cultures (HAEC).** A) HAEC
621 were pretreated with 1000 U/mL IFN- α basolaterally for 2 hours prior to and during infection.
622 Cultures were then infected apically with influenza A/California/09 H1N1 virus or SARS-CoV-2.
623 Apical washes were collected at the indicated times and progeny titers determined by plaque
624 assay on MDCK cells (influenza virus) or Vero E6 cells (SARS-CoV-2). At the 48 h endpoint,
625 cultures were lysed for western blot analysis. B) Western for total STAT1 or phospho-STAT1 at
626 48 hpi, and actin as loading control. C) Influenza A virus titers by plaque assay on MDCK cells.

627 0 h, virus inoculate; 2 h, virus in third apical wash; 8, 24, 48 h, virus in apical washes at these
628 time points. D) SARS-CoV-2 titers by plaque assay on Vero E6 cells. 0 h, virus inoculate; 2 h,
629 virus in second apical wash; 8, 24, 48 h, virus in apical washes at these time points.

630 **Figure 4, SARS-CoV-2 impacted by post IFN-I treatment.** A-B) Vero E6 and Calu3 2B4 cells
631 were infected with either SARS-CoV WT (black) or SARS-CoV-2 (blue) at an MOI 0.01 (A, Vero
632 cells) or MOI 1 (B, Calu3 cells). Cells were subsequently treated with 1000 U/mL recombinant
633 type I IFN (hashed line) or mock (solid line) for 4 hours following infection. Each point on the line
634 graph represents the group mean, $N \geq 3$. All error bars represent SD. The two tailed student's t-
635 test was used to determine P-values: **P < 0.01 *** P < 0.001.

636 **Figure 5, Conservation of SARS-CoV IFN antagonists.** Viral protein sequences of the
637 indicated viruses were aligned according to the bounds of the SARS-CoV open reading frames
638 for each viral protein. Sequence identities were extracted from the alignments for each viral
639 protein, and a heat map of percent sequence identity was constructed using EvolView
640 (www.evolgenius.info/evolview) with SARS-CoV as the reference sequence. TR = truncated
641 protein.

642

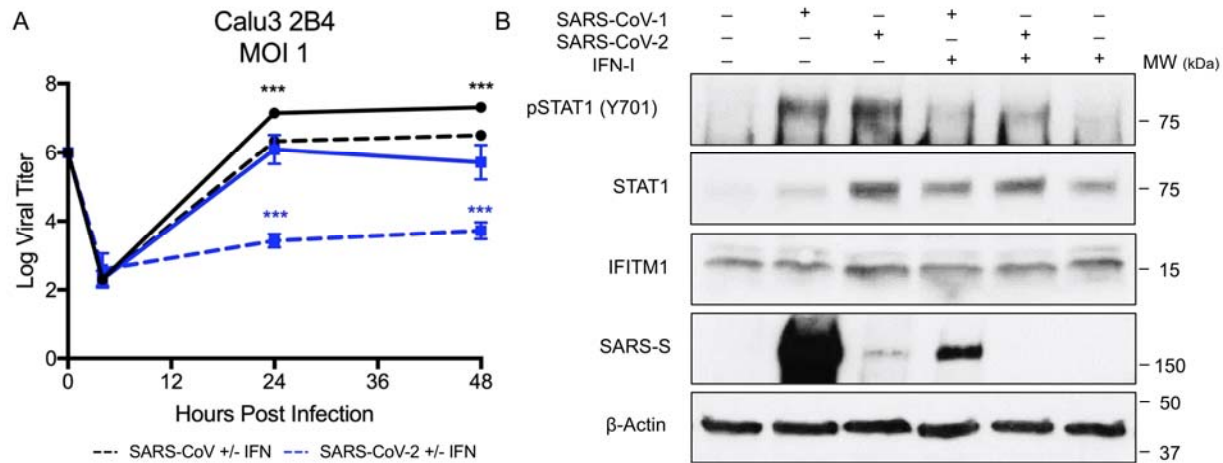


643

644

645 **Figure 1. SARS-CoV-2 sensitive to type I IFN pretreatment.** A) Vero E6 cells were treated
646 with 1000 U/mL recombinant type I (hashed line) IFN or mock (solid line) for 18 hours prior to
647 infection. Cells were subsequently infected with either SARS-CoV WT (black) or SARS-CoV-2
648 (blue) at an MOI of 0.01 as described above. Each point on the line graph represents the group
649 mean, $N \geq 3$. All error bars represent SD. The two tailed student's t-test was used to determine
650 P-values: *** $P < 0.001$. B) Vero cell protein lysates from IFN-I treated and untreated cells were
651 probed 48 hours post infection by Western blotting for phosphorylated STAT1 (Y701), STAT1,
652 IFITM1, SARS spike, and Actin.
653

654

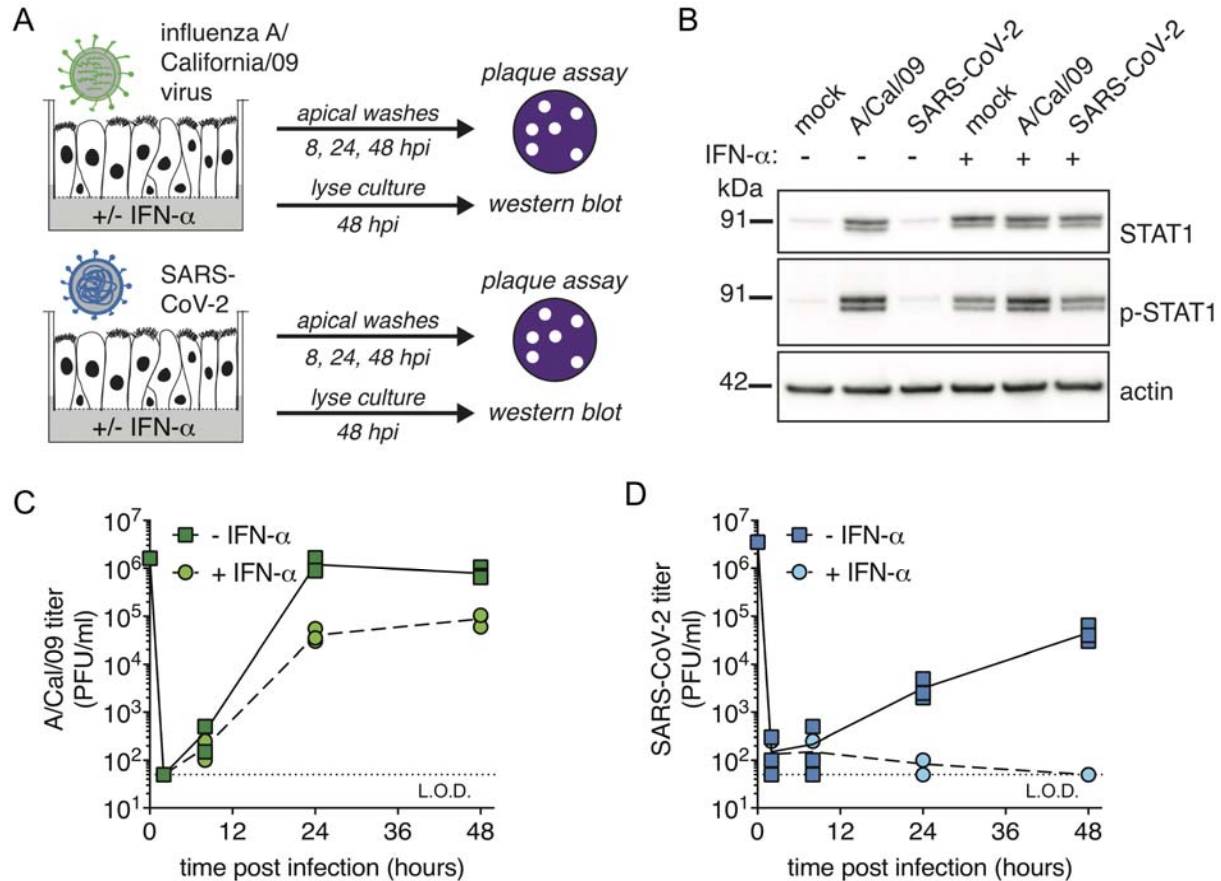


655

656

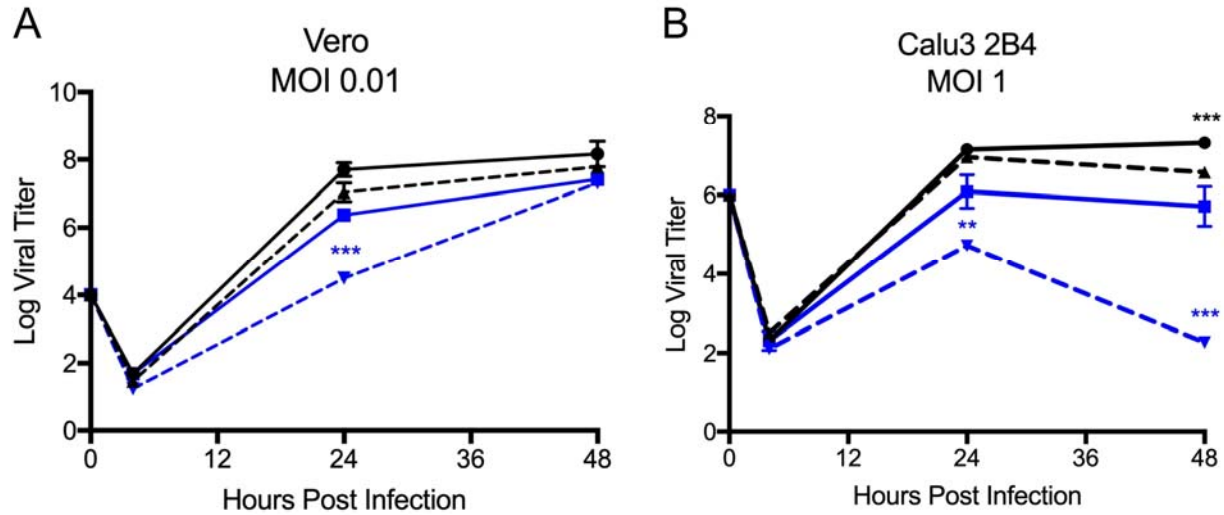
657 **Figure 2. SARS-CoV-2 attenuated and IFN-I sensitive in Calu3 respiratory cells.** A) Calu3
658 2B4 cells were treated with 1000 U/mL recombinant type I (hashed line) IFN or mock (solid line)
659 for 18 hours prior to infection. Cells were subsequently infected with either SARS-CoV WT
660 (black) or SARS-CoV-2 (blue) at an MOI of 1. Each point on the line graph represents the
661 group mean, N ≥ 3. All error bars represent SD. The two tailed student's t-test was used to
662 determine P-values: *** P < 0.001. B) Calu3 cell protein lysates from IFN-I treated and untreated
663 cells were probed 48 hours post infection by Western blotting for phosphorylated STAT1 (Y701),
664 STAT1, IFITM1, SARS spike, and Actin.

665



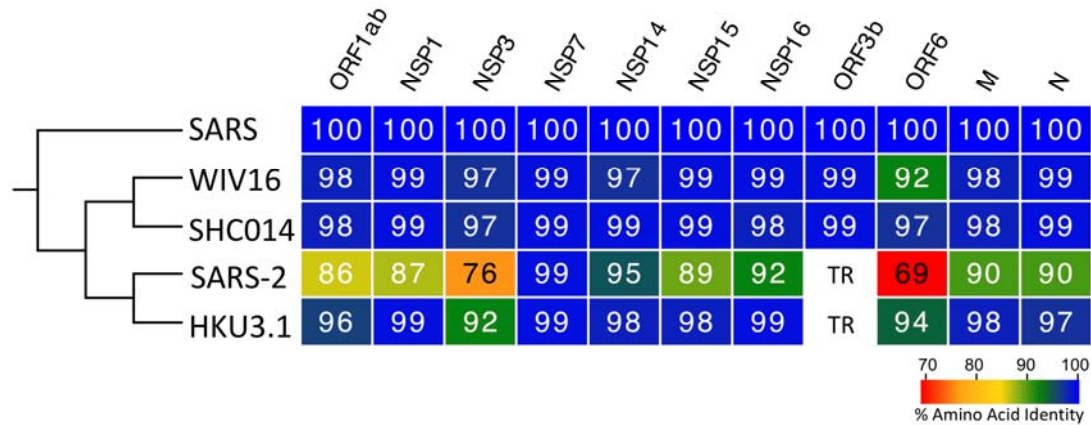
666
667

668 **Figure 3. Differential IFN-I sensitivity and pSTAT1 phosphorylation following SARS-CoV-**
 669 **2 or influenza A virus on polarized human airway epithelial cultures (HAEC).** A) HAEC
 670 were pretreated with 1000 U/mL IFN- α basolaterally for 2 hours prior to and during infection.
 671 Cultures were then infected apically with influenza A/California/09 H1N1 virus or SARS-CoV-2.
 672 Apical washes were collected at the indicated times and progeny titers determined by plaque
 673 assay on MDCK cells (influenza virus) or Vero E6 cells (SARS-CoV-2). At the 48 h endpoint,
 674 cultures were lysed for western blot analysis. B) Western for total STAT1 or phospho-STAT1 at
 675 48 hpi. C) Influenza A virus titers by plaque assay on MDCK cells. 0 h, virus inoculate; 2 h, virus
 676 in third apical wash; 8, 24, 48 h, virus in apical washes at these time points. D) SARS-CoV-2
 677 titers by plaque assay on Vero E6 cells. 0 h, virus inoculate; 2 h, virus in second apical wash; 8,
 678 24, 48 h, virus in apical washes at these time points.
 679



680
681
682
683
684
685
686

Figure 4, SARS-CoV-2 impacted by post IFN-I treatment. A-B) Vero E6 and Calu3 2B4 cells were infected with either SARS-CoV WT (black) or SARS-CoV-2 (blue) at an MOI 0.01 (A, Vero cells) or MOI 1 (B, Calu3 cells). Cells were subsequently treated with 1000 U/mL recombinant type I IFN (hashed line) or mock (solid line) for 4 hours following infection. Each point on the line graph represents the group mean, $N \geq 3$. All error bars represent SD. The two tailed student's t-test was used to determine P-values: **P < 0.01 *** P < 0.001.



687

688 **Figure 5, Conservation of SARS-CoV IFN antagonists.** Viral protein sequences of the
 689 indicated viruses were aligned according to the bounds of the SARS-CoV open reading frames
 690 for each viral protein. Sequence identities were extracted from the alignments for each viral
 691 protein, and a heat map of percent sequence identity was constructed using EvolView
 692 (www.evolgenius.info/evolview) with SARS-CoV as the reference sequence. TR = truncated
 693 protein.